Evolution of genetic (co)variances during the worldwide invasion of *Drosophila suzukii*

Antoine Fraimout[1†], Stéphane Chantepie[1], Nicolas Navarro[2], Céline Teplitsky[3]* and Vincent Debat[1]*

Short title: Quantitative genetics of *Drosophila suzukii* wing shape

[1]Institut de Systématique, Evolution, Biodiversité, ISYEB – CNRS, MNHN, UPMC, EPHE, Université des Antilles, Muséum National d'Histoire Naturelle, Sorbonne Universités, 45 rue Buffon, 75005 Paris, France
[2]UMR CNRS 6282 Biogéosciences, Université de Bourgogne-Franche-Comté, 21000 Dijon, France
[3]Centre d'Ecologie Fonctionnelle et Evolutive, CEFE – UMR 5175 – CNRS, IRD, EPHE, Université de Montpellier, Université Paul Valéry, 34293 Montpellier, France

[†]Corresponding author, E-mail: fraimout.antoine@gmail.com

*These authors contributed equally to this work

Abstract

Biological invasions offer particularly convenient situations to study phenotypic evolution in natural populations. In particular, the comparison of derived, invasive populations with ancestral extant populations allows to investigate the relative impact of neutral demographic events, genetic constraints and selection on the evolution of phenotypes. In this paper, focusing on the worldwide invasion of *Drosophila suzukii* (Matsumara, 1931), we investigate how phenotypic divergence among populations is constrained by the genetic correlations summarized in the genetic covariance matrix **G** and how **G** itself evolves throughout periods of drift and selection. Leveraging invasion history resolved by population genetics approaches, we compared wing shape **G** matrices among ancestral native and derived invasive populations, contrasting patterns of quantitative divergence among populations to neutral expectations. Our results show moderate yet significant quantitative genetic differentiation of wing shape among *D. suzukii* populations and a relative stability in the structure of **G**, presenting a roughly spherical shape but slightly different volumes. These characteristics likely reflect the demographic history of populations and suggest a low level of genetic constraint on adaptive evolution. The divergence among populations was greater than expected under a purely neutral model of evolution, compatible with an effect of selection on wing shape. Overall, our study suggests that selection, drift but not constraints affected the early stages of wing shape evolution during *D. suzukii* invasion.

Key words: *Drosophila suzukii*, **G**-matrix, geometric morphometrics, biological invasion, quantitative genetics, Q_{ST}-F_{ST}

Introduction

Biological invasions often involve stochastic demographic changes through founder effects and genetic bottlenecks (Golani *et al.*, 2007) or the shuffling of different alleles by genetic admixture between populations (Rius & Darling, 2014). Invasive populations can also be subjected to multiple and often new selective pressures in the new environment and throughout the invasion process (Kilkenny & Galloway, 2013). Consequently, they tend to show marked genetic and phenotypic differences compared to their source populations, and distinguishing whether this differentiation results from adaptive or neutral evolution is challenging (Lee, 2002; Wares, 2005; Facon *et al.*, 2006; Hayes & Barry, 2008; Keller & Taylor, 2008; Prentis *et al.*, 2008; Bock *et al.*, 2015; Dlugosch *et al.*, 2015; Estoup *et al.*, 2016). Furthermore, these evolutionary changes can happen over relatively short time scales (Colautti & Lau, 2015). Hence, a topical question in invasion biology is how fast can invasive populations evolve in their new environment? Can we detect adaptive evolution occurring at the onset of the invasion (Szucs *et al.*, 2017) ?

Multivariate phenotypic evolution depends on the variances and covariances of the traits (Lande, 1976), summarized in **G**, the genetic variance-covariance matrix. In particular, the orientation of genetic (co)variance between traits relatively to the direction of selection applied will condition the phenotypic response to selection (Arnold *et al.*, 2001), either constraining or facilitating it, thereby affecting the pace of adaptive evolution (Agrawal & Stinchcombe, 2009; Fischer *et al.*, 2016). This is formalized in the multivariate breeder's equation (Lande, 1979):

$$R = G\beta$$

where the response to selection R equals the product of **G** and the directional selection gradient β. It has been proposed in the context of evolutionary diversification, that the **G** matrix of an ancestral population can constrain derived populations to diverge along certain directions of the phenotypic space (*i.e.* the lines of least evolutionary resistance; Schluter, 1996). Nevertheless, valid predictions of evolutionary trajectories depend on whether or not **G** remains stable across space and time (Jones *et al.*, 2004; Arnold *et al.*, 2008). The stability of **G** has received much attention (*e.g.* Roff, 2000; Steppan *et al.*, 2002; Bégin & Roff, 2003; Mezey & Houle, 2003; Björklund, 2004; Blows & Hoffmann, 2005; Arnold *et al.*, 2008; Walsh & Blows, 2009) and its sensitivity to selection, migration and drift has been investigated both theoretically (*e.g.* Jones *et al.*, 2004; Guillaume & Whitlock, 2007, Chantepie & Chevin, 2020), and empirically under natural and laboratory

conditions (Merilä *et al.*, 1994; Phillips *et al.*, 2001; Conner *et al.*, 2003; Cano *et al.*, 2004; Eroukhmanoff. & Svensson, 2011; Bjorklund *et al.*, 2013; McGlothlin *et al.*, 2018; Walter 2023). Multiple lines of evidence suggest that the structure of **G** can be altered by selection (Jones *et al.*, 2003; Jones *et al.*, 2004; Dugand *et al.* 2021), drift (Phillips *et al.*, 2001) and environmental conditions (*e.g.* Sikkink *et al.*, 2015; Wood & Brodie, 2015) even over the span of a single generation (Siren *et al.*, 2017). However, there is also recent evidence for stable **G** matrices across populations and continents (*e.g.*, Puentes *et al.*, 2016; Delahaie *et al.*, 2017) and overall, the stability of **G** cannot be taken for granted and requires additional empirical evaluation.

Here, we focus on the worldwide invasion of the spotted wing drosophila, *Drosophila suzukii* (Matsumura, 1931) to assess the stability of **G** between native and invasive populations across continents and test the effect of genetic constraints upon phenotypic divergence. *Drosophila suzukii* is a highly invasive pest of agricultural crops in Europe and North America where it was first detected almost simultaneously in 2008 (see Asplen *et al.*, 2015 for review). We reconstructed the detailed history of this worldwide invasion and showed the presence of multiple independent introductions from Asia involving population bottlenecks and genetic admixture events within invaded regions (Fraimout *et al.*, 2017). A consequence of this complex history is that native and invasive populations show significant levels of neutral genetic differentiation as measured by F_{ST} estimated using microsatellite loci (Fraimout *et al.*, 2015; Fraimout *et al.*, 2017). At the phenotypic level, we showed using laboratory lines derived from a sample of natural populations that native and invasive *D. suzukii* display genetically based differences in wing shape and size (Fraimout *et al.*, 2018).

This invasion provides an opportune model to address long standing questions about (1) the evolution of genetic variances and covariances in natural populations and (2) their consequences on traits' evolution. First, the worldwide geographic distribution of *D. suzukii* allows to investigate the stability of **G** across multiple populations with specific histories of invasion. We expect that periods of bottlenecks and population admixture – all experienced by invasive *D. suzukii* populations to a different extent (Fraimout *et al.*, 2017, Olzacuaga *et al.* 2020) – may have altered the structure of **G** in invasive populations. Specifically, depletion of genetic variance due to bottlenecks, or new combinations of alleles produced by genetic admixture, could affect the volume or shape **G** (*i.e.,* the amount and distribution of genetic variance over the first axes of variation). Our first objective was thus to investigate whether or not **G** remained stable throughout the complex demographic history of *D. suzukii*'s invasion. Second, by sampling flies shortly after the invasion occurred (*i.e.*,

approximately 6 years after detection) makes it possible to investigate the early stages of phenotypic divergence between extant ancestral (*i.e.* native) and derived (*i.e.* invasive) populations. We aimed at testing predictions from quantitative genetic theory regarding the effect of selection or drift on the phenotypic divergence among invasive populations. For instance, early stages of adaptive phenotypic divergence could be constrained by the direction of the major axis of the ancestral **G** matrix (*i.e.* **g**max of native Asian populations; Schluter, 1996; McGuigan, 2006; Walter *et al.*, 2018) and result in an alignment between **g**max and the leading vector of divergence. On the other hand, under a neutral model of phenotypic evolution, divergence among populations (**D**) is expected to take place along the axis of greatest genetic variation (Lande 1979) and to be proportional to the genetic variance in **G** (Chenoweth *et al.* 2010). In other words, a concordance between the major axes of **D** and **G** could also be suggestive of population differentiation resulting mainly from neutral evolution (Arnold *et al.* 2001; Bégin & Roff, 2003) while deviation from this pattern could be indicative of selection acting on the wing shape of *D. suzukii*. Our second objective was thus to shed light on the possible role of selection or drift on the evolution of wing shape in invasive *D. suzukii* populations by assessing the relationship between the matrix of among-populations divergence **D** and the ancestral **G** matrix (Begin & Roff 2003).

We used an isofemale line breeding design (Hoffmann & Parsons, 1988; David *et al.*, 2005; Berger *et al.*, 2013) and a geometric morphometric approach to estimate the quantitative genetic divergence in wing shape between six natural populations of *D. suzukii* sampled in the native area (Japan) and the two main invaded areas in Europe and the USA. We specifically addressed the following questions: i) how did wing shape evolve across multiple invasive populations? ii) are there structural differences in **G** among all populations? iii) can phenotypic divergence among invasive populations be attributed to selection acting on wing shape?

Material and methods

Samples, lines and data acquisition

Drosophila suzukii adults were sampled in 2014 using banana bait traps and net swiping at six localities representative of their global distribution range in Japan (native range), USA and France (invasive range) (Fig. 1). Within each country we sampled two localities representative of a northern and a southern latitude. Repeated clinal evolution of wing morphology has been described in the related invasive species *Drosophila*

subobscura and proposed as an adaption to different temperature optima at northern and southern latitudes (Huey *et al.*, 2000; Gilchrist *et al.*, 2001; Gilchrist *et al.*, 2004). Thus, we hypothesized that sampling populations close to the extremes of their latitudinal distribution would maximize our chance to capture phenotypic and possibly, adaptive, divergence in the invaded range. In USA and France, these localities were also representative of the invasion history with the southern locality corresponding to the first reported occurrence of *D. suzukii* (Watsonville, USA and Montpellier, France; Hauser, 2011; Calabria *et al.*, 2012) and the northern locality representing the expansion front of the species in the area at the time of sampling (Dayton, Oregon, USA and Paris, France). It is worth stressing that although the most likely genetic source populations of Europe and USA invasions were identified in continental Asia (*i.e.* China, Fraimout *et al.*, 2017), *F* statistics and Bayesian clustering methods indicate weak differentiation between these sources and our Japanese population samples, thereby suggesting that the use of Japanese populations as ancestral representatives is an acceptable approximation. For the Japanese flies, a northern population was sampled in Sapporo (Hokkaido island) and a southern population was sampled in Tokyo (Honshu island). In both Japanese localities, traps were placed in gardens inside the university campuses. In the invasive north American range sampling habitats corresponded to vineyards in Dayton, and strawberry fields in Watsonville. French samples were collected in the botanical garden of the Natural History Museum in Paris and close to vineyards in Montpellier. An average of 30 isofemale lines (see Table. S1 for details and population codes) were established for each locality by placing randomly chosen wild-caught gravid females in separate rearing vials, and splitting F_1 offsprings in five replicate vials. Following the isofemale approach, we further expanded each line by letting individuals mate freely within tubes (*i.e.*, full-sib mating) and transferring their progeny to new rearing vials each generation. We repeated this for five generations and at the fifth generation, a single female per line was isolated in a new rearing tube to produce the focal offspring used in the study. At the end of the experiment, 5 to 10 full-sib males were randomly chosen from each line from each population for phenotyping. Rearing medium consisted of corn-starch and yeast with added anti-biotic (hydroxy-4 benzoate). Lines were randomly positioned in incubators and kept for the five generations at 22°C. A total of 1323 individuals distributed across 177 isofemale lines were phenotyped. Wings were carefully clipped from over-anesthetized flies using tweezers and mounted on glass slides in a mixture of ethanol and glycerin. Coverslips were sealed using nail polish and maintained with small weights to flatten the wing as much as possible. Images of the wings were

acquired with a Leica DFC 420 digital camera mounted on a Leica Z6 APO microscope. Fifteen landmarks were defined on the dorsal side of the right wing and digitized using a custom *ImageJ* plugin written by C. P. Klingenberg (pers. comm.).

Wing shape differentiation – Geometric morphometric analyses

Procrustes generalized least squares superimposition was used to extract shape information from the landmarks coordinates (GLS, *e.g.* Dryden & Mardia, 1993). Shape data have been used in multiple quantitative genetics studies (Klingenberg & Leamy, 2001; Klingenberg, 2003; Monteiro *et al.*, 2003; Hansen *et al.*, 2004; Mezey & Houle, 2005; Myers *et al.*, 2006; Polly, 2008; Klingenberg, 2010; Adams, 2011; Leinonen *et al.*, 2011; Martínez-Abadías *et al.*, 2012) and are suitable for the estimation of **G**. A principal component analysis (PCA) was first applied to the set of 30 coordinates and the non-null 26 components were conserved as input data. Centroid size was used as a size variable in the subsequent analyses and compared between all pairs of populations. As divergence in wing shape first appeared to be weak on PCA plot we further performed a between-group principal component analysis (*bgPCA*) to visualize the overall variation in wing shape among populations (*e.g.* Mitteroecker & Bookstein, 2011). We then estimated the statistical significance of the shape divergence among populations by applying a multivariate analysis of variance (MANOVA) with the 26 PCs as response variable and population of origin as a fixed effect. We further estimated the pairwise differences among populations with permutational pairwise MANOVAs, using the *RVAideMemoire* R package (v.0.9-55, Hervé, 2016). We used the Wilk's test statistic and set the number of permutations to 10000 while correcting for multiple testing using the *fdr* method (Benjamini & Hochberg 1995). To account for allometric relationship within and between populations, we also fitted the MANOVAs using the residuals of the size/shape regressions.

Wing shape differentiation – phenotypic divergence vector analysis

We further estimated differentiation in wing shape by calculating vectors of phenotypic divergence among populations (*e.g.,* Stuart *et al.* 2017, Fraimout *et al.* 2022b). Specifically, we were interested in quantifying the phenotypic divergence of each invasive population from a hypothetical native ancestor. To do so, the phenotypic mean of each population was estimated from multivariate linear models (MANOVA) using the 26 non-null PC representative of wing shape and accounting for differences in wing size by adding the wing

centroid size as covariate. Then, we estimated the differences between each invasive population mean wing shape, and the mean wing shape calculated from both Japanese populations. We also estimated divergence at the country level by estimating the difference between the mean ancestral (Japanese) wing shape and the mean wing shape of USA and France populations, respectively. In total, we obtained 6 phenotypic divergence vectors describing the difference between the ancestral Japanese and each invasive population (4 vectors) and between the ancestor and each country's mean wing shape (2 vectors). We then assessed the similarity between these vectors of divergence by comparing their angle to the distribution of angles between 10,000 pairs of random vectors of the same dimensionality (Klingenberg and McIntyre, 1998). This allowed us to test whether phenotypic divergence occurred in similar or different directions in the phenotypic space, and whether any two vectors were more similar or different than expected by chance. Angles between vectors were calculated as:

$$\alpha = \cos^{-1}(\Delta z_{Di}, \Delta z^{T}_{Dj}) \quad [1]$$

where z_D corresponds to a divergence vector of population *i* or *j* from the ancestor. An eigenanalysis of the four population vectors was applied to synthetize the main axes of divergences.

*Matrices estimations – population-specific **G** matrices*

We estimated the six **G** matrices corresponding to the six sampled populations under a Bayesian framework using the R-package *MCMCglmm* (Hadfield, 2010). To this end, we partitioned the phenotypic variance in wing shape for each population using a multivariate animal model (Kruuk, 2004) of the form:

$$y = \sum X\beta + \sum Z\gamma + \varepsilon \quad [2]$$

where y is the multivariate vector of phenotypic values for wing shape corresponding to the 26 non-null principal components (PCs) accounting for the totality of shape variance; β is the vector of fixed effect; γ is the vector of random effects; ε is the vector of residual errors and X and Z the design matrices relating to the fixed and random effects, respectively. We estimated **G** matrices separately for each population using model [2] and appended the matrix of relatedness between individuals to the vector of random effects with the *pedigree* option implemented in the *MCMCglmm* function. The pedigree corresponding to our crossing design was coded in R using custom scripts (see *Data availability* statement). In all models, wing centroid size was fitted as covariate. We used a prior set with variance estimates following a 'broken-stick' model of decrease of variance, appropriate for the use of PC scores representing decreasing proportion of explained variance

(Jolliffe, 2002), with null covariances and a degree of belief *nu* = n + 0.002 (where n is the number of traits, Houle & Meyer, 2015). We ran each model for 1 200 000 iterations with a burnin period of 200 000 and a thinning rate of 1000, resulting in 1000 Monte Carlo Markov Chain (MCMC) posterior samples. The convergence of models was checked visually from plots of MCMC chains and posterior distributions as well as autocorrelation level (<0.05 in all models). All analyses were performed in R (v.4.2.2; R Core Team, 2022).

*Matrices comparisons – Differences in the size and shape of **G***

For each pairwise comparison of **G** matrices between populations, we estimated which aspect of the structure of **G** differed between populations by computing the size and shape of the matrices (Robinson & Beckerman, 2013; Teplitsky *et al.*, 2014). Matrix size (*i.e.* volume) was calculated as the sum of the matrix eigenvalues. We estimated the shape of the matrix by its eccentricity, (*i.e.* the ratio of the first, to the second eigenvalue; Jones *et al.*, 2003). Additionally, to the matrices' shape we also estimated the difference in the proportion of variance along $\mathbf{g}_{max}$ for each pairwise comparisons of **G**. Significance of metric differences between populations was assessed by estimating the ratio between each population metrics and examining the overlap between the 95% highest posterior density (HPD) of these ratios calculated from the MCMC posterior samples with zero.

Matrices comparisons – Genetic covariance tensor

We further tested for differences among our set of **G** matrices by following the approach of Hine *et al.* (2009) and Aguirre *et al.* (2014) using a fourth-order genetic covariance tensor analysis (hereafter 'covariance tensors'). Briefly (see details in Hine *et al.* 2009; Aguirre *et al.* 2014), variances and covariances among all elements of the original set of **G** matrices are calculated to construct the fourth-order covariance tensor **Σ** and the second-order (*i.e.* matrix) tensor **S**. Eigenanalysis of the **S**-matrix allows for the construction of eigentensors which represent independent vectors of differences in variance and covariance among **G** matrices. Covariance tensors provide a way to compare more than two genetic covariance matrices and describe independent axes of divergence among them. In other words, covariance tensors allow to identify trait combinations explaining most genetic variation among **G** matrices. We applied the covariance tensor analysis to our set of six **G** matrices using the full 1000 MCMC samples for each matrix and compared the observed

divergence to the null expectation obtained from the analyses of random **G** matrices. We used an approach based on Morrissey *et al.* (2019) to simulate the null distribution of **G** matrix. Briefly, for each population, the breeding values of founders were drawn from a multivariate distribution with zero mean and a variance-covariance matrix equal to the **G**-matrix estimated from this population with the animal model [2]. Breeding values were then randomly shuffled among the founders and the breeding values of all remaining individuals were estimated based on the pedigree of each population. The breeding values of an individual were drawn from a multivariate normal distribution with a vector of means equal to the mean breeding values of its parents and a deviation equal to the segregation variance (Walsh & Lynch, 2018). For an individual, the segregation variance was estimated as half the product of the randomized **G** matrix of their population (estimated on the new population's founders) and one minus the average inbreeding coefficient of its parents (Walsh & Lynch, 2018, pp.557). The phenotypes were then recomposed by adding the random and fixed effects estimated by the animal model following [2]

We repeated this sequence for each posterior sample of animal models and resulted in 1000 null datasets for each population. The **G** matrix of null datasets was estimated following eq. [2]. To reduce computational burden, we sampled 200 posterior samples for each null animal model (Morrissey *et al*., 2019) to compute a mean null distribution **G** matrix for each population, that accounts for both the sampling effect and the uncertainty in the **G** matrix estimates. Each final null **G** matrix consisted of the average of the 1000 MCMC posterior for each of the 100 replicates and were used to estimate random genetic covariance tensor as described in Aguirre *et al.* (2014) using custom scripts in R (see *Data availability* section for source code),

*Test of selection: similarity between **G** and **D***

It has been suggested that the adaptive phenotypic divergence among a set of derived populations can be biased along the directions of greatest genetic variation of the common ancestral population, resulting in a close similarity between the ancestral **G** matrix and the matrix of populations divergence (**D**) Schluter 1996).

The similarity between **D** and **G** was first investigated by computing the angle between a divergence vector ***d*** and the ancestral **G** matrix following Krzanowski (1979):

$$\theta = cos^{-1}\{(dLL^t d^t)^{-0.5}\}$$

, where **L** is the set of first q eigenvectors of **G**, where q was set equal to half the shape space dimensionality ($q = (2k - 4)/2 = 13$; and k is the number of digitized landmarks). We compared the observed angles to their random expectations by simulating 1000 random vectors v_{2k} projected in the tangent space according to

$$d = (I_{2k} - \mu\mu^t)v$$

where $\boldsymbol{\mu}$ is the vectorised mean shape (Dryden and Mardia, 1998). However, it was shown that drift might also induce proportionality between **G** and **D** (Lande *et al.* 1979; McGuigan *et al.* 2005), pointing at the need of a more stringent test to decipher the adaptive and neutral scenarios (Martin *et al*. 2008).

We thus followed the two steps method proposed by Martin *et al.* (2008). First, the coefficient of proportionality ρ_{ST} between the ancestral **G** matrix and the divergence matrix **D** was estimated and compared to the predicted neutral divergence $2F_{ST}/(1-F_{ST})$ obtained from neutral molecular markers (Rogers and Harpending 1983; Martin et al 2008). Deviation from this value would be indicative of selection. Second, proportionality between **D** and **G** was tested using the MANOVA estimates of the covariance matrices. We used the *k.prop* R function of the neutrality package from Martin *et al.* (2008) to calculate ρ_{ST} and the *hierfstat* R package (v.0.5.11; Goudet & Jombart 2022) to get bootstrapped estimates of F_{ST} from 25 neutral microsatellite loci (Fraimout *et al.* 2015, 2017). We then used the Bartlett-adjusted test of proportionality as recommended in Martin *et al.* (2008). Inputs for both tests were obtained by performing a MANOVA on the wing shape data and using the log-centroid size as covariate and population of origin as fixed effect. Also following recommendation from the authors, we used the first 11 PCs describing wing shape variation to maximise accuracy of the statistical tests so that $p < 2nb$ (where p is the number of traits and nb is the number of populations sampled) while retaining PCs accounting for > 90% of variance.

Test of selection: solving the multivariate breeder's equation

The hypothesis that selection may have been involved in the divergence of wing shapes among populations was further explored using the multivariate breeder's equation (Lande 1979). First, an experimental selection differential was derived from data obtained in a previous study of the effects of temperature on *D. suzukii* wing morphology and flight performance (Fraimout *et al.*, 2018). In this previous study, we reconstructed 3D flight trajectories of flies reared under different developmental temperatures and measured flight parameters such as

speed, acceleration, or sinuosity. Recorded individual wings were digitized and wing landmarks coordinates used to assess the relationship between flight parameters and wing shape. Landmark data of this previous study were aligned onto the reference configuration of the present study to allow direct comparability. Hypothesizing that flight performance might significantly contribute to fitness (e.g. Frazier et al. 2008), the shape change associated with the strongest flight speed difference was used as a hypothetical selection differential. Wing shape was regressed onto the log of flight speed using a multivariate regression (*e.g.* Mardia *et al.* 1979; Monteiro 1999) to estimate the vector of shape change associated with highest flight velocity s_{velocity}. The corresponding response to selection Δz was then predicted using the multivariate breeder's equation (Lande and Arnold 1983) and the estimated ancestral (*i.e.* Japanese) **G** and **P** matrices:

$$\Delta z = G_{jap} P_{jap}^{-} s_{velocity}$$

where $^{-}$ is the Moore-Penrose generalized inverse. This predicted response to velocity selection was compared to the different vectors of population divergences (see above) by computing the angle between them following

$$\alpha = cos^{-1} \frac{\Delta z}{\|\Delta z\|} \cdot \frac{d^t}{\|d\|}$$

The observed angles were then compared to the expectation of the angle between Δz and 1000 random vectors (see above). Our hypothesis here is that if wing shape associated with higher flight speed would be a target of selection, we should observe a match between the evolutionary shape changes (the phenotypic divergence among populations) and the shape change resulting from the hypothetical response to selection.

Test of selection: percentage of genetic variance along divergence vectors

Finally, we reasoned that if selection was involved in the short-term evolution of wing shape, it should manifest in a depletion of genetic variation in the selected directions (*e.g.* Agrawal and Stinchcombe 2009), corresponding to the directions of divergence from the hypothetical common ancestor. To test this prediction, **G** matrices of each population were projected onto the shape space directions defined by the divergence vectors, $d^t G d$, and expressed in proportion of the total genetic variance. The amount of genetic variance in the direction defined by ***d*** was then compared between the ancestral and derived **G** matrices. We predicted that a reduction in this proportion of variance should be detected if selection was involved in the evolutionary

divergence. To test whether these amount of variance along those directions were lower than expected by chance, we estimated the amount of variance given a series of random vectors previously projected onto the tangent space (see above).

Results

Significant divergence of wing size and shape across populations

We observed differentiation in wing centroid size between American and all other populations, as well as between the two American populations (Fig. S1): the American populations displayed smaller wing size, with US-WAT displaying the smallest wings. Although the divergence for wing shape among populations was weak, the *bgPCA* showed a signal of geographic differentiation, opposing the pairs of populations according to their geographic origin (Fig. S2). This shape divergence was confirmed by the significant population effect in the MANOVA (Wilk's lambda = 0.143, df = 5, $p < 0.001$). The MANOVA performed on the residuals of the regression between shape and size also revealed a significant population effect (Wilk's lambda = 0.199, df = 5, $p < 0.001$), suggesting that the shape difference goes beyond a simple allometric effect. The pairwise permutational MANOVAs revealed significant shape differences between all pairs of populations ($p < 1e\text{-}04$). The analysis of the angles between the divergence vectors suggests that both French populations present a rather similar divergence from their common ancestor, more similar than two random vectors ($\alpha = 31.9°$, $p < 10^{-4}$, Fig. 2, Table S2). For the American populations, this divergence was more heterogeneous and the angle between the two divergence vectors was greater than that of the French populations ($\alpha = 49.9°$, $p = 5 \times 10^{-4}$, Fig 2, Table S2). The average American and French divergences were strikingly different, and no more similar than random vectors ($\alpha = 71.9°$, $p = 0.11$, Table S2). The American populations appeared slightly less divergent than French populations, based on the Procrustes distance from their hypothetical ancestor (5.72×10^{-3}, 7.46×10^{-3}, respectively; Table S3) and as observed from the *bgPCA* (Fig. S2).

*The **G**-matrix for wing shape is mostly stable across populations*

We found significant differences in the size of the **G** matrix among 3 pairs of populations, all involving the southern USA population US-WAT (Table 1). The **G** matrix of the US-WAT population had a significantly

higher volume than those of US-DAY (northern USA) and both French populations (FR-PAR and FR-MON). All other pairwise comparisons did not reveal significant differences in the volumes of **G**. Eccentricity values for all matrices were spanning over 1.5 (Fig. S3) indicating relative sphericity. However, we did not find significant differences in the shape of the **G** matrices as eccentricity and the amount of variance explained by $\boldsymbol{g}_{max}$ between any pairs of populations were not statistically different (Fig. S3).

We found no significant difference between the eigentensors of **S** calculated from the set of random and observed set of **G** matrices based on the overlapping 95% HPD intervals (Fig. 3A). We further projected the six **G** matrices in the space of the first eigentensor (**E**1) and found no significant differences between populations (Fig. 3B). Investigation of the proportion of additive genetic variance (V_A) along the leading eigenvector of **E**1 ($e_{11;}$ Fig.3C) showed similar results to the volume analysis with a trend for higher V_A for the US-WAT compared to both French populations and the US-DAY population. While this trend could be compatible with the effect of admixture in US-WAT and bottlenecks in US-DAY, FR-MON and FR-PAR, the observed differences were not statistically significant.

The divergence matrix D is proportional to the ancestral G matrix: an effect of selection?

Overall, the divergence matrix appeared fairly similar to the ancestral **G** matrix, its first two PCs and the ancestral **G** matrix respectively forming narrow angles of 13.6 and 15.8°, smaller than expected with random vectors (47.9°± 7.18). The divergence between populations thus tended to follow the lines of genetic least resistance, as expected under both neutral and selective scenarios. While the null hypothesis of proportionality between both matrices was not rejected (Bartlett-adjusted X^2 test; $p = 1$), suggesting a close match, the coefficient of proportionality ($\rho = 1.063$; 95% CI, 0.763 – 1.751) was in turn higher than the coefficient estimated for microsatellite markers ($2F_{ST}/(1-F_{ST}) = 0.160$; 95% CI, 0.128 – 0.198) Therefore, while **D** and **G** are proportional, their coefficient of proportionality deviates from the neutral expectation, suggesting a role for selection in the observed divergence.

No reduction in genetic variance in the direction of divergence

We further projected each **G** matrix onto their respective direction of divergence from the hypothetical ancestor and estimated the corresponding percentage of variance (Fig. 4). Overall, we found that amounts of genetic

variance in these directions were not statistically different among populations. Furthermore, we did not observe lower amount of genetic variance between the projection of each population **G** matrix and the projection of the ancestral **G** matrix on their corresponding divergence vectors. This result goes against our expectation that selection would result in a depletion of genetic variance along each population's divergence vector from the ancestor.

The response to a theoretical selection does not match the observed divergences

To investigate the possible selective factors affecting wing shape evolution in *D. suzukii* invasion, we simulated the evolutionary responses to a hypothetical selection differential, the wing shape difference between high and slow *D. suzukii* flyers, as reported in Fraimout *et al.* (2018; Fig. 5a). The evolutionary response is shown on Fig. 5b, as the average response derived from the full posterior of MCMC samples. The shape divergence of French and American populations from their common hypothetical ancestor are shown on Figure 5c and d (the two Japanese populations used to compute the ancestral **G** matrix were considered too close from this ancestral state and were thus not considered). The pattern of shape change associated with $\boldsymbol{S}_{velocity}$ and the average response Δz were very similar (mean α = 22.74°, SD 6.03) suggesting that **G** and **P** do not strongly constrain the response to selection. This result was in line with the fact that we found the ancestral **G** matrix to have a relative spherical shape, which should therefore not constrain the response to selection. While a similarity in the shift of the basal landmarks can be found between the divergence of French populations and the theoretical response to selection, no obvious similarity with American populations divergences is detected (Fig 5b,c,d, Fig. S4). However, this congruence was not reflected in the correlation between vectors when accounting for the full landmark configurations as the evolution of the distal part of the wing did not match the expected response to selection (Fig. 5b, c, Fig. S4). Overall, the similarity between the divergence vectors from each population and the response to selection Δz was low (Fig. S4) suggesting that the observed divergence in wing shape does not result from selection on faster flight capacity.

Discussion

Population differentiation of Drosophila suzukii wing shape

Geographical variation of wing morphology has been described in several *Drosophila* species (*e.g.* Azevedo

et al., 1998; Haas & Tolley, 1998; Hoffmann & Shirriffs, 2002), including introduced ones (Huey *et al.*, 2000). In particular, geographical clines of wing size and shape have been detected along latitudinal and altitudinal gradients (Huey *et al.* 2000, Gilchrist *et al.* 2004; Gilchrist *et al.*, 2001; Gilchrist *et al.*, 2004; Pitchers *et al.*, 2013; Adrion *et al.*, 2015). These clines have typically been interpreted as adaptations to flight conditions, specifically temperature and air pressure (Dillon and Frazier 2006; Pitchers et al 2013), although direct evidence on the nature of selection is lacking. In *D. suzukii*, clines in wing morphology have been reported along an altitudinal gradient in Hawaii – the first and oldest invaded territory (Asplen *et al.*, 2015) – with flies from high altitude (ca. 2000m) displaying significantly larger wings than flies sampled at sea level (Koch *et al.*, 2020). Here, we detected a geographic divergence of wing shape across all populations, but the differences among north and south populations were different among continents. Gilchrist *et al.* (2000) reported comparable differences in latitudinal wing shape changes in *D. melanogaster* from three continents, and suggested the occurrence of specific local selective pressures on wing shape. However, they also detected parallel clines in wing size across continents, suggesting common adaptive effects. In our study, wing size was more stable: the only difference between northern and southern populations was found in the USA. As for wing shape, although we found that populations from the same continent have evolved differences in a relatively similar direction of the phenotypic space, we did not find any evidence for parallel latitudinal clines. At the time of sampling, the invasion of *D. suzukii* was initiated less than a decade ago in Europe and the USA and it is possible that adaptive geographical clines did not have enough time to evolve in these regions, contrary to the first invaded range in Hawaii (Koch *et al.* 2020). As a comparison, a latitudinal cline in *D. subobscura* following colonization of the New World, was reported after two decades, while no difference had been detected ten years after the start of the invasion (Huey *et al.*, 2000; Gilchrist *et al.*, 2004). At this point, it is unclear whether *D. suzukii* wing phenotypes are locally adapted, and additional work is warranted to decipher the interplay between wing plasticity, genetics and their association with fitness in natural *D. suzukii* populations. Nevertheless, by rearing flies in controlled laboratory conditions for a few generations, we showed that the phenotypic divergence observed among populations is genetically based rather than plastically induced (see also Fraimout *et al* 2018) and that some evolutionary process independent of phenotypic plasticity have shaped the wing of *D. suzukii* in the wild.

*Evolution of the **G** matrix*

Despite intense theoretical and empirical research (e.g. Roff, 2000; Steppan *et al.*, 2002; Bégin & Roff, 2003; Jones *et al.*, 2003; Mezey & Houle, 2003; Björklund, 2004; Jones *et al.*, 2004; Blows & Hoffmann, 2005; Arnold *et al.*, 2008; Walsh & Blows, 2009; Jones *et al.*, 2014; Wood & Brodie, 2015; Puentes *et al.*, 2016; Svensson *et al.*, 2021), predicting how natural selection or drift will affect the structure of **G** and at which pace **G** can evolve in the wild remains a difficult task. As stated by Jones *et al.* (2003): "[...] *the current state of analytical theory on **G**-matrix evolution is that existing theory cannot guarantee stability of the **G**-matrix (Turelli 1988), but also does not guarantee instability*." Following this assertion, simulation studies (Jones *et al.*, 2003; Jones *et al.*, 2004; Arnold *et al.*, 2008; Jones *et al.*, 2014; Björklund & Gustafsson, 2015; Chantepie & Chevin 2020) have identified how correlative selection, pleiotropic mutations, population size and other evolutionary forces can affect the stability of **G**'s structure and orientation. However, empirically and 20 years later, evidence for both stability (Delahaie *et al.*, 2017; McGlothlin *et al.*, 2018) and instability (*e.g.*, Uesugi *et al.*, 2017) have been reported in varying contexts.

Here we found that the **G** matrices were globally stable across populations, the differences between populations principally pertaining to the volume of **G** (i.e. the global amount of genetic variance.) Specifically, French populations seemed to display less genetic variance as indicated by their smaller volumes, while the US-WAT population seemed more genetically variable than the rest of the populations. Reduction of genetic variance and, therefore, of the volume of **G**, is expected under certain conditions such as reduced population size and increased genetic drift (Shaw *et al.*, 1995; Roff, 2000; Jones *et al.*, 2003; Jones *et al.*, 2004). According to the results of Fraimout *et al.* (2017) obtained from neutral molecular markers and more recently from Olazcuaga *et al.* (2020) using whole-genome data, all invasive populations of *D. suzukii* experienced significant loss of genetic diversity due to various intensities of bottlenecks upon introduction. Lesser levels of genetic variance and lower volumes in the French **G** matrices are thus consistent with the effect of drift. Similarly, the higher volume of the US-WAT population could be explained by genetic admixture of two highly differentiated lineages (Fraimout *et al.* 2017). However, populations' invasion history was not reflected in all **G** matrices as other genetically admixed populations (FR-PAR, US-DAY; Fraimout *et al.* 2017) did not show higher volumes and neither did ancestral populations where genetic bottlenecks most likely did not occur. Contrasting with the random evolution of **G** in all directions of the multivariate space expected under genetic drift (Arnold *et al.*,

2001; Phillips *et al.*, 2001), our results show that most aspects of the eigenstructure of **G** (size and shape) have remained stable throughout the invasion process.

Adaptive or neutral divergence?

We tested the hypotheses of neutral or adaptive evolution by estimating the similarity between the ancestral **G** matrix and the divergence matrix **D**, and found that the leading vectors of both matrices were tightly associated. Such similarity is compatible with a neutral divergence because genetic drift is expected to induce divergence along the axes with the most genetic variation, and proportionally to the amount of variation in the ancestral population (Lande 1979; Lofsvold 1998; Marroig and Cheverud, 2004). However, this pattern is also expected under selection, if applied on the main directions of genetic variation (*i.e.* the lines of genetic least resistance; Schluter, 1996). Our estimation of the coefficient of proportionality supports this second hypothesis, as it was significantly greater than expected under neutral divergence. The divergence in wing shape among invasive populations of *D. suzukii* might thus be adaptive. The statistical power of this test is conditional on the sampling design and particularly the number of populations sampled (Martin *et al.* 2008). While the test for departure of neutrality should be robust to small number of populations (*i.e.,* < 10 as in the current study) results of the proportionality test should be interpreted with caution. Similar analyses using long-diverged groups (*i.e.,* Teosinte and Maize), report values of ρ_{ST} several order of magnitude above the neutral expectation (Yang *et al.* 2019), suggesting that the signal of selection we observe in *D. suzukii* is rather low.

We then leveraged available flight data to test the hypothesis that selection on flight speed could be involved in this divergence. We computed the response to selection of the ancestral **G** matrix by applying a selection differential corresponding to flight speed differences (Fraimout *et al.* 2018). Despite partial correspondence of the predicted response to selection with the observed evolutionary divergence, the similarity was insufficient to conclude that flight speed had been a target of selection throughout the invasion of *D. suzukii*. The factors involved in selection on *D. suzukii* wing shape thus remain to be identified.

Conclusion

Consensual predictions on the effect of selection and drift on the **G** matrix remain scarce in the literature and most empirical evidence are based on experimental evolution studies (*e.g.* Doroszuk *et al.*, 2008; Careau *et al.*,

2015) or comparisons among long-diverged species (e.g. McGlothlin *et al.*, 2018). In this context our study provides new insights on the evolution (or lack thereof) of **G** over a relatively short evolutionary time scale in natural conditions. We showed that native and invasive populations of *D. suzukii* display quantitative genetic differentiation in wing shape across continents and at an early stage of their worldwide invasion. Our results suggest an effect of selection acting on a poorly constraining ancestral G matrix. They provide a reference point for future studies quantifying phenotypic evolution in this species.

Acknowledgments

AF was supported by the Agence Nationale de la Recherche, through the LabEx ANR-10-LABX-0003-BCDiv, of the program "Investissements d'avenir" (ANR-11-IDEX-0004-02). VD was funded by ANR SWING (ANR-16- CE02-0015). The authors are grateful to S. Fellous, A. Xuéreb, K. Tamura, M. Toda, P. Shearer, T. Schlenke and A. Kopp for help with flies sampling. We thank M. Guillaume for helping with the stock flies maintenance and F. Peronnet for providing flies rearing medium.

Author contribution

AF, VD and CT designed the study; AF, SC and NN analyzed the data; AF and VD obtained the samples; AF led the writing of the first draft and all authors contributed critically to the manuscript.

Data availability

Data and code necessary to replicate the analyses presented in the manuscript are available from github (github.com/afraimout/).

References

Adams, D. C., Otárola-Castillo, E. J. M. i. E., & Evolution. (2013). geomorph: an R package for the collection and analysis of geometric morphometric shape data. *4*(4), 393-399.

Adams, D. C. J. E. B. (2011). Quantitative genetics and evolution of head shape in Plethodon salamanders. *38*(3), 278.

Adrion, J. R., Hahn, M. W., & Cooper, B. S. (2015). Revisiting classic clines in Drosophila melanogaster in the age of genomics. *Trends in Genetics, 31*(8), 434-444.

Agrawal, A. F., & Stinchcombe, J. R. (2009). How much do genetic covariances alter the rate of adaptation? *Proc Biol Sci, 276*(1659), 1183-1191. doi:10.1098/rspb.2008.1671

Arnold, S. J., Burger, R., Hohenlohe, P. A., Ajie, B. C., & Jones, A. G. (2008). Understanding the

evolution and stability of the G-matrix. *Evolution, 62*(10), 2451-2461. doi:10.1111/j.1558-5646.2008.00472.x

Arnold, S. J., Pfrender, M. E., & Jones, A. G. (2001). The adaptive landscape as a conceptual bridge between micro-and macroevolution *Microevolution Rate, Pattern, Process* (pp. 9-32): Springer.

Asplen, M. K., Anfora, G., Biondi, A., Choi, D.-S., Chu, D., Daane, K. M., Gibert, P., Gutierrez, A. P., Hoelmer, K. A., Hutchison, W. D.*, et al.* (2015). Invasion biology of spotted wing Drosophila (Drosophila suzukii): a global perspective and future priorities. *Journal of Pest Science, 88*(3), 469-494. doi:10.1007/s10340-015-0681-z

Azevedo, R. B., James, A. C., McCabe, J., & Partridge, L. J. E. (1998). Latitudinal variation of wing: thorax size ratio and wing-aspect ratio in Drosophila melanogaster. *52*(5), 1353-1362.

Bégin, M., & Roff, D. A. (2003). The Constancy of the G Matrix through Species Divergence and the Effects of Quantitative Genetic Constraints on Phenotypic Evolution: A Case Study in Crickets. *Evolution, 57*(5). doi:10.1554/0014-3820(2003)057[1107:Tcotgm]2.0.Co;2

Berger, D., Postma, E., Blanckenhorn, W. U., & Walters, R. J. (2013). Quantitative genetic divergence and standing genetic (co)variance in thermal reaction norms along latitude. *Evolution, 67*(8), 2385-2399. doi:10.1111/evo.12138

Björklund, M. (2004). Constancy of the G Matrix in Ecological Time. *Evolution, 58*(6). doi:10.1554/03-410

Björklund, M., & Gustafsson, L. J. E. (2015). The stability of the G-matrix: The role of spatial heterogeneity. *69*(7), 1953-1958.

Bjorklund, M., Husby, A., & Gustafsson, L. (2013). Rapid and unpredictable changes of the G-matrix in a natural bird population over 25 years. *Journal of Evolutionary Biology, 26*(1), 1-13.

Blows, M. W., & Hoffmann, A. A. (2005). A reassessment of genetic limits to evolutionary change. *Ecology, 86*(6), 1371-1384.

Bock, D. G., Caseys, C., Cousens, R. D., Hahn, M. A., Heredia, S. M., Hubner, S., Turner, K. G., Whitney, K. D., & Rieseberg, L. H. (2015). What we still don't know about invasion genetics. *Molecular Ecology, 24*(9), 2277-2297. doi:10.1111/mec.13032

Calabria, G., Máca, J., Bächli, G., Serra, L., & Pascual, M. (2012). First records of the potential pest species Drosophila suzukii (Diptera: Drosophilidae) in Europe. *Journal of Applied Entomology, 136*(1-2), 139-147. doi:10.1111/j.1439-0418.2010.01583.x

Cano, J. M., Laurila, A., Palo, J., & Merilä, J. J. E. (2004). Population differentiation in G matrix structure due to natural selection in Rana temporaria. *58*(9), 2013-2020.

Careau, V., Wolak, M. E., Carter, P. A., & Garland, T. J. P. R. S. B. (2015). Evolution of the additive genetic variance–covariance matrix under continuous directional selection on a complex behavioural phenotype. *282*(1819), 20151119.

Chantepie, S., & Chevin, L. M. (2020). How does the strength of selection influence genetic correlations?. Evolution letters, 4(6), 468-478.

Colautti, R. I., & Lau, J. A. J. M. E. (2015). Contemporary evolution during invasion: evidence for differentiation, natural selection, and local adaptation. *24*(9), 1999-2017.

Conner, J. K., Franks, R., & Stewart, C. (2003). Expression of additive genetic variances and covariances for wild radish floral traits: comparison between field and greenhouse environments. *Evolution, 57*(3), 487-495.

Crnokrak, P., Merilä, J. J. T. i. E., & Evolution. (2002). Genetic population divergence: markers and traits. *17*(11), 501.

David, J., Gibert, P., Legout, H., Pétavy, G., Capy, P., & Moreteau, B. J. H. (2005). Isofemale lines in Drosophila: an empirical approach to quantitative trait analysis in natural populations. *94*(1), 3.

Delahaie, B., Charmantier, A., Chantepie, S., Garant, D., Porlier, M., & Teplitsky, C. (2017). Conserved G-matrices of morphological and life-history traits among continental and island

blue tit populations. *Heredity (Edinb), 119*(2), 76-87. doi:10.1038/hdy.2017.15

Dlugosch, K. M., Anderson, S. R., Braasch, J., Cang, F. A., & Gillette, H. D. (2015). The devil is in the details: genetic variation in introduced populations and its contributions to invasion. *Molecular Ecology, 24*(9), 2095-2111. doi:10.1111/mec.13183

Doroszuk, A., Wojewodzic, M. W., Gort, G., & Kammenga, J. E. (2008). Rapid divergence of genetic variance-covariance matrix within a natural population. *American Naturalist, 171*(3), 291-304. doi:10.1086/527478

Dryden, I. L., & Mardia, K. V. J. S. T. I. J. o. S., Series A. (1993). Multivariate shape analysis. 460-480.

Eroukhmanoff., & Svensson, E. I. (2011). Evolution and stability of the G-matrix during the colonization of a novel environment. *Journal of Evolutionary Biology, 24*(6), 1363-1373. doi:10.1111/j.1420-9101.2011.02270.x

Estoup, A., Ravigné, V., Hufbauer, R., Vitalis, R., Gautier, M., & Facon, B. (2016). Is There a Genetic Paradox of Biological Invasion? *Annual Review of Ecology, Evolution, and Systematics, 47*(1), 51-72. doi:10.1146/annurev-ecolsys-121415-032116

Facon, B., Genton, B. J., Shykoff, J., Jarne, P., Estoup, A., & David, P. (2006). A general eco-evolutionary framework for understanding bioinvasions. *Trends in Ecology & Evolution, 21*(3), 130-135. doi:10.1016/j.tree.2005.10.012

Fischer, E. K., Ghalambor, C. K., & Hoke, K. L. (2016). Plasticity and evolution in correlated suites of traits. *Journal of Evolutionary Biology, 29*(5), 991-1002. doi:10.1111/jeb.12839

Fraimout, A., Debat, V., Fellous, S., Hufbauer, R. A., Foucaud, J., Pudlo, P., Marin, J.-M., Price, D. K., Cattel, J., Chen, X. J. M. b*., et al.* (2017). Deciphering the routes of invasion of Drosophila suzukii by means of ABC random forest. *34*(4), 980-996.

Fraimout, A., Jacquemart, P., Villarroel, B., Aponte, D. J., Decamps, T., Herrel, A., Cornette, R., & Debat, V. J. J. o. E. B. (2018). Phenotypic plasticity of Drosophila suzukii wing to developmental temperature: implications for flight. *221*(13), jeb166868.

Fraimout, A., Loiseau, A., Price, D. K., Xuereb, A., Jean-Francois, M., Vitalis, R., Fellous, S., Debat, V., & Estoup, A. (2015). New set of microsatellite markers for the spotted-wing Drosophila suzukii (Diptera: Drosophilidae): A promising molecular tool for inferring the invasion history of this major insect pest. *European Journal of Entomology, 112*(4), 855-859. doi:10.14411/eje.2015.079

Gilchrist, G. W., Huey, R. B., Balanyà, J., Pascual, M., & Serra, L. (2004). A Time Series of Evolution in Action: A Latitudinal Cline in Wing Size in South American Drosophila Subobscura. *Evolution, 58*(4). doi:10.1554/03-414

Gilchrist, G. W., Huey, R. B., & Serra, L. (2001). Rapid evolution of wing size clines in Drosophila subobscura *Microevolution Rate, Pattern, Process* (pp. 273-286): Springer.

Golani, D., Azzurro, E., Corsini-Foka, M., Falautano, M., Andaloro, F., & Bernardi, G. J. B. l. (2007). Genetic bottlenecks and successful biological invasions: the case of a recent Lessepsian migrant. *3*(5), 541-545.

Goudet, J., & Martin, G. J. G. (2007). Under neutrality, QST<= FST when there is dominance in an island model.

Guillaume, F., & Whitlock, M. C. J. E. I. J. o. O. E. (2007). Effects of migration on the genetic covariance matrix. *61*(10), 2398-2409.

Haas, H. L., & Tolley, K. A. J. J. o. Z. (1998). Geographic variation of wing morphology in three Eurasian populations of the fruit fly, Drosophila lummei. *245*(2), 197-203.

Hadfield, J. D. (2010). MCMC methods for multi-response generalized linear mixed models: the MCMCglmm R package. *Journal of Statistical Software, 33*(2), 1-22.

Hansen, T. F., Houle, D. J. P. i. S. t. e., & phenotypes, e. o. c. (2004). Evolvability, stabilizing selection, and the problem of stasis. 130-150.

Hauser, M. (2011). A historic account of the invasion of Drosophila suzukii (Matsumura) (Diptera:

Drosophilidae) in the continental United States, with remarks on their identification. *Pest Manag Sci, 67*(11), 1352-1357. doi:10.1002/ps.2265

Hayes, K. R., & Barry, S. C. (2008). Are there any consistent predictors of invasion success? *Biological Invasions, 10*(4), 483-506.

Hervé, M. (2016). RVAideMemoire: diverse basic statistical and graphical functions. R package v 0.9-55.

Hoffmann, A., & Parsons, P. J. G., selection, evolution. (1988). The analysis of quantitative variation in natural populations with isofemale strains. *20*(1), 87.

Hoffmann, A. A., & Shirriffs, J. J. E. (2002). Geographic variation for wing shape in Drosophila serrata. *56*(5), 1068-1073.

Houle, D., & Meyer, K. J. J. o. e. b. (2015). Estimating sampling error of evolutionary statistics based on genetic covariance matrices using maximum likelihood. *28*(8), 1542-1549.

Huey, R. B., Gilchrist, G. W., Carlson, M. L., Berrigan, D., & Serra, L. J. S. (2000). Rapid evolution of a geographic cline in size in an introduced fly. *287*(5451), 308-309.

Jolliffe, I. T. J. P. c. a. (2002). Graphical representation of data using principal components. 78-110.

Jones, A. G., Arnold, S. J., & Burger, R. (2004). Evolution and Stability of the G-Matrix on a Landscape with a Moving Optimum. *Evolution, 58*(8). doi:10.1554/03-651

Jones, A. G., Arnold, S. J., & Bürger, R. J. E. (2003). Stability of the G-matrix in a population experiencing pleiotropic mutation, stabilizing selection, and genetic drift. *57*(8), 1747-1760.

Jones, A. G., Bürger, R., & Arnold, S. J. (2014). Epistasis and natural selection shape the mutational architecture of complex traits. *Nature communications, 5*(1), 1-10.

Karhunen, M., Merilä, J., Leinonen, T., Cano, J., & Ovaskainen, O. J. M. E. R. (2013). driftsel: an R package for detecting signals of natural selection in quantitative traits. *13*(4), 746-754.

Keller, S. R., & Taylor, D. R. J. E. L. (2008). History, chance and adaptation during biological invasion: separating stochastic phenotypic evolution from response to selection. *11*(8), 852-866.

Kilkenny, F. F., & Galloway, L. F. (2013). Adaptive divergence at the margin of an invaded range. *Evolution, 67*(3), 722-731. doi:10.1111/j.1558-5646.2012.01829.x

Klingenberg, C. P., & Leamy, L. J. J. E. (2001). Quantitative genetics of geometric shape in the mouse mandible. *55*(11), 2342-2352.

Klingenberg, C. P. J. E. (2003). Quantitative genetics of geometric shape: heritability and the pitfalls of the univariate approach. *57*(1), 191-195.

Klingenberg, C. P. J. N. R. G. (2010). Evolution and development of shape: integrating quantitative approaches. *11*(9), 623.

Koch, J. B., Dupuis, J. R., Jardeleza, M.-K., Ouedraogo, N., Geib, S. M., Follett, P. A., & Price, D. K. (2020). Population genomic and phenotype diversity of invasive Drosophila suzukii in Hawai ‘i. *Biological Invasions*, 1-18.

Kruuk, L. E. J. P. T. o. t. R. S. o. L. S. B. B. S. (2004). Estimating genetic parameters in natural populations using the ‘animal model’. *359*(1446), 873-890.

Lande, R. J. E. (1976). Natural selection and random genetic drift in phenotypic evolution. *30*(2), 314-334.

Lande, R. J. E. (1979). Quantitative genetic analysis of multivariate evolution, applied to brain: body size allometry. *33*(1Part2), 402-416.

Le Roy, C., Debat, V., & Llaurens, V. J. B. R. (2019). Adaptive evolution of butterfly wing shape: from morphology to behaviour. *94*(4), 1261-1281.

Lee, C. E. (2002). Evolutionary genetics of invasive species. *Trends in Ecology & Evolution, 17*(8), 386-391.

Leinonen, T., Cano, J. M., & Merila, J. (2011). Genetics of body shape and armour variation in threespine sticklebacks. *Journal of Evolutionary Biology, 24*(1), 206-218. doi:10.1111/j.1420-9101.2010.02161.x

Leinonen, T., McCairns, R. S., O'hara, R. B., & Merilä, J. (2013). QST–FST comparisons: evolutionary and ecological insights from genomic heterogeneity. *Nature Reviews Genetics, 14*(3), 179.

Lynch, M., & Walsh, B. (1998). *Genetics and Analysis of Quantitative Traits*: Sinauer.

Martínez-Abadías, N., Mitteroecker, P., Parsons, T. E., Esparza, M., Sjøvold, T., Rolian, C., Richtsmeier, J. T., & Hallgrímsson, B. J. E. b. (2012). The developmental basis of quantitative craniofacial variation in humans and mice. *39*(4), 554-567.

Matsumura, S. (1931). 6000 illustrated insects of Japan-Empire, 1931, 8+ 1497-I-23 pp., 10 pis: Tokyo.

McGlothlin, J. W., Kobiela, M. E., Wright, H. V., Mahler, D. L., Kolbe, J. J., Losos, J. B., & Brodie, E. D., 3rd. (2018). Adaptive radiation along a deeply conserved genetic line of least resistance in Anolis lizards. *Evol Lett, 2*(4), 310-322. doi:10.1002/evl3.72

McGuigan, K. J. M. e. (2006). Studying phenotypic evolution using multivariate quantitative genetics. *15*(4), 883-896.

Merila, J., Bjorklund, M., & Gustafsson, L. (1994). Evolution of Morphological Differences with Moderate Genetic Correlations among Traits as Exemplified by 2 Flycatcher Species (Ficedula, Muscicapidae). *Biological Journal of the Linnean Society, 52*(1), 19-30.

Merilä, J., & Crnokrak, P. (2001). Comparison of genetic differentiation at marker loci and quantitative traits. *Journal of Evolutionary Biology, 14*(6), 892-903.

Mezey, J. G., & Houle, D. (2003). Comparing G matrices: Are common principal components informative? *Genetics, 165*(1), 411-425.

Mezey, J. G., & Houle, D. J. E. (2005). The dimensionality of genetic variation for wing shape in Drosophila melanogaster. *59*(5), 1027-1038.

Mitteroecker, P., & Bookstein, F. (2011). Linear Discrimination, Ordination, and the Visualization of Selection Gradients in Modern Morphometrics. *Evolutionary Biology, 38*(1), 100-114. doi:10.1007/s11692-011-9109-8

Monteiro, L. R., Duarte, L. C., & dos Reis, S. F. (2003). Environmental correlates of geographical variation in skull and mandible shape of the punar rat Thrichomys apereoides (Rodentia: Echimyidae). *Journal of Zoology, 261*(1), 47-57. doi:10.1017/s0952836903003893

Morrissey, M. B., Hangartner, S., & Monro, K. (2019). A note on simulating null distributions for G matrix comparisons. Evolution, 73(12), 2512-2517.

Myers, E. M., Janzen, F. J., Adams, D. C., & Tucker, J. K. J. E. (2006). Quantitative genetics of plastron shape in slider turtles (Trachemys scripta). *60*(3), 563-572.

Olazcuaga, L., Loiseau, A., Parrinello, H., Paris, M., Fraimout, A., Guedot, C., ... & Gautier, M. (2020). A whole-genome scan for association with invasion success in the fruit fly Drosophila suzukii using contrasts of allele frequencies corrected for population structure. Molecular biology and evolution, 37(8), 2369-2385.

Ovaskainen, O., Karhunen, M., Zheng, C., Arias, J. M. C., & Merilä, J. J. G. (2011). A new method to uncover signatures of divergent and stabilizing selection in quantitative traits. *189*(2), 621-632.

Perrings, C., Dehnen-Schmutz, K., Touza, J., & Williamson, M. (2005). How to manage biological invasions under globalization. *Trends in Ecology & Evolution, 20*(5), 212-215. doi:10.1016/j.tree.2005.02.011

Phillips, P. C., Whitlock, M. C., & Fowler, K. J. G. (2001). Inbreeding changes the shape of the genetic covariance matrix in Drosophila melanogaster. *158*(3), 1137-1145.

Pitchers, W., Pool, J. E., & Dworkin, I. J. E. I. J. o. O. E. (2013). Altitudinal clinal variation in wing size and shape in African Drosophila melanogaster: one cline or many? *, 67*(2), 438-452.

Polly, P. D. J. E. b. (2008). Developmental dynamics and G-matrices: can morphometric spaces be used to model phenotypic evolution? *, 35*(2), 83.

Prentis, P. J., Wilson, J. R., Dormontt, E. E., Richardson, D. M., & Lowe, A. J. (2008). Adaptive

evolution in invasive species. *Trends in Plant Science, 13*(6), 288-294. doi:10.1016/j.tplants.2008.03.004

Puentes, A., Granath, G., & Agren, J. (2016). Similarity in G matrix structure among natural populations of Arabidopsis lyrata. *Evolution, 70*(10), 2370-2386. doi:10.1111/evo.13034

Rius, M., & Darling, J. A. (2014). How important is intraspecific genetic admixture to the success of colonising populations? *Trends in Ecology & Evolution, 29*(4), 233-242. doi:10.1016/j.tree.2014.02.003

Robinson, M. R., & Beckerman, A. P. (2013). Quantifying multivariate plasticity: genetic variation in resource acquisition drives plasticity in resource allocation to components of life history. *Ecology Letters, 16*(3), 281-290. doi:10.1111/ele.12047

Roff, D. J. H. (2000). The evolution of the G matrix: selection or drift? *, 84*(2), 135-142.

Rogers, A. R., & Harpending, H. C. (1983). Population structure and quantitative characters. Genetics, 105(4), 985-1002.

Schafer, M. A., Berger, D., Rohner, P. T., Kjaersgaard, A., Bauerfeind, S. S., Guillaume, F., Fox, C. W., & Blanckenhorn, W. U. (2018). Geographic clines in wing morphology relate to colonization history in New World but not Old World populations of yellow dung flies. *Evolution*. doi:10.1111/evo.13517

Schluter, D. J. E. (1996). Adaptive radiation along genetic lines of least resistance. *50*(5), 1766-1774.

Shaw, F. H., Shaw, R. G., Wilkinson, G. S., & Turelli, M. J. E. (1995). Changes in genetic variances and covariances: G whiz! *, 49*(6), 1260-1267.

Sikkink, K. L., Reynolds, R. M., Cresko, W. A., & Phillips, P. C. (2015). Environmentally induced changes in correlated responses to selection reveal variable pleiotropy across a complex genetic network. *Evolution, 69*(5), 1128-1142. doi:10.1111/evo.12651

Siren, J., Ovaskainen, O., & Merila, J. (2017). Structure and stability of genetic variance-covariance matrices: A Bayesian sparse factor analysis of transcriptional variation in the three-spined stickleback. *Molecular Ecology, 26*(19), 5099-5113. doi:10.1111/mec.14265

Steppan, S. J., Phillips, P. C., Houle, D. J. T. i. E., & Evolution. (2002). Comparative quantitative genetics: evolution of the G matrix. *17*(7), 320-327.

Svensson, E. I., Arnold, S. J., Bürger, R., Csilléry, K., Draghi, J., Henshaw, J. M., Jones, A. G., De Lisle, S., Marques, D. A., & McGuigan, K. (2021). Correlational selection in the age of genomics. *Nature Ecology and Evolution*, 1-12.

Szucs, M., Vahsen, M. L., Melbourne, B. A., Hoover, C., Weiss-Lehman, C., & Hufbauer, R. A. (2017). Rapid adaptive evolution in novel environments acts as an architect of population range expansion. *Proc Natl Acad Sci U S A, 114*(51), 13501-13506. doi:10.1073/pnas.1712934114

Teplitsky, C., Robinson, M. R., & Merilä, J. J. Q. g. i. t. w. (2014). Evolutionary potential and constraints in wild populations. 190-208.

Uesugi, A., Connallon, T., Kessler, A., & Monro, K. (2017). Relaxation of herbivore-mediated selection drives the evolution of genetic covariances between plant competitive and defense traits. *Evolution, 71*(6), 1700-1709.

Walsh, B., & Blows, M. W. (2009). Abundant Genetic Variation plus Strong Selection = Multivariate Genetic Constraints: A Geometric View of Adaptation. *Annual Review of Ecology Evolution and Systematics, 40*, 41-59.

Walsh, B., & Lynch, M. (2018). Evolution and selection of quantitative traits. Oxford University Press.

Walter, G. M., Aguirre, J. D., Blows, M. W., & Ortiz-Barrientos, D. (2018). Evolution of Genetic Variance during Adaptive Radiation. *American Naturalist, 191*(4), E108-E128. doi:10.1086/696123

Walter, G. M. (2023). Experimental evidence that phenotypic evolution but not plasticity occurs along genetic lines of least resistance in homogeneous environments. The American Naturalist,

201(4), E70-E89.
Wares, J. (2005). Mechanisms that drive evolutionary change. Insights from species introduction and invasions. *Species invasions: insights into ecology, evolution, and biogeography*, 229-257.
Whitlock, M. C. (2008). Evolutionary inference from QST. *Molecular Ecology, 17*(8), 1885-1896. doi:10.1111/j.1365-294X.2008.03712.x
Wood, C. W., & Brodie, E. D., 3rd. (2015). Environmental effects on the structure of the G-matrix. *Evolution, 69*(11), 2927-2940. doi:10.1111/evo.12795

FIGURES AND TABLES

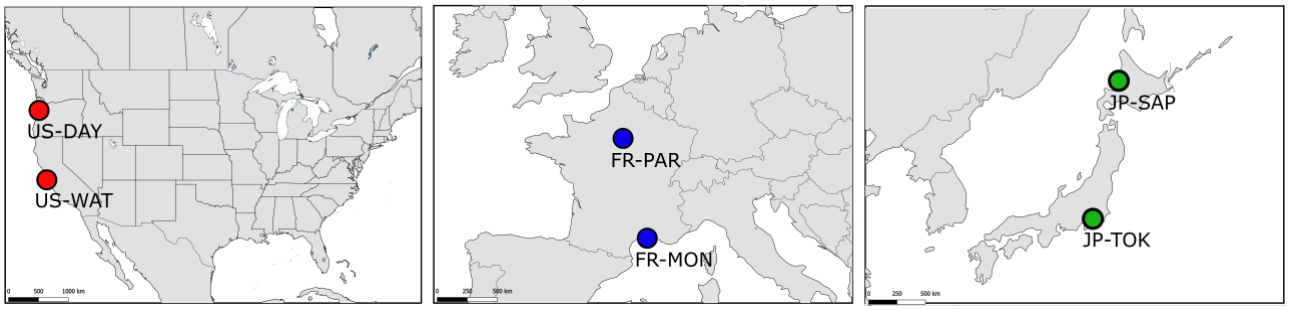

Figure 1. Sampling locations of the six *D. suzukii* populations. Adult *D. suzukii* were sampled from the wild in 3 countries (dark grey shading) from the native range in Japan (green circles) and the invasive range in France (blue circles) and the USA (red circles).

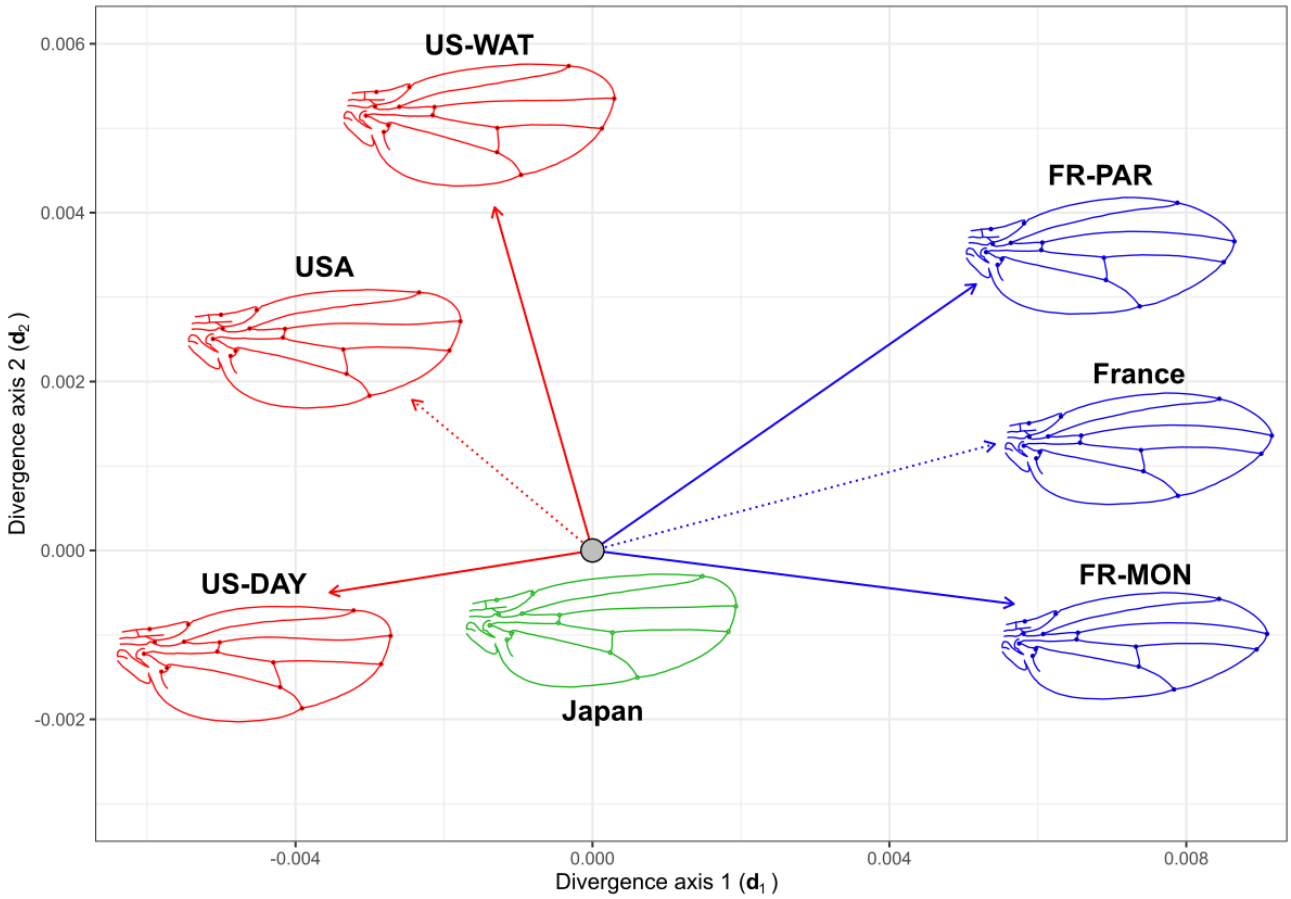

Figure 2. Phenotypic divergence of the invasive populations from their common ancestor. Graphical representation of the vectors of phenotypic divergence of each invasive population (solid line) from their hypothetical common ancestor (Japan, grey filled circle). The vectors are projected on the multivariate divergence space where d1 and d2 represent the first and second main axes of the multivariate divergent covariance matrix. The divergence vectors of the corresponding country matrices (dashed lines) are also shown. Colors correspond to Japanese (green), French (blue) and American (red) matrices. Wing shape outlines represent the mean shape of each group and show the wing shape evolution from the Japanese ancestor.

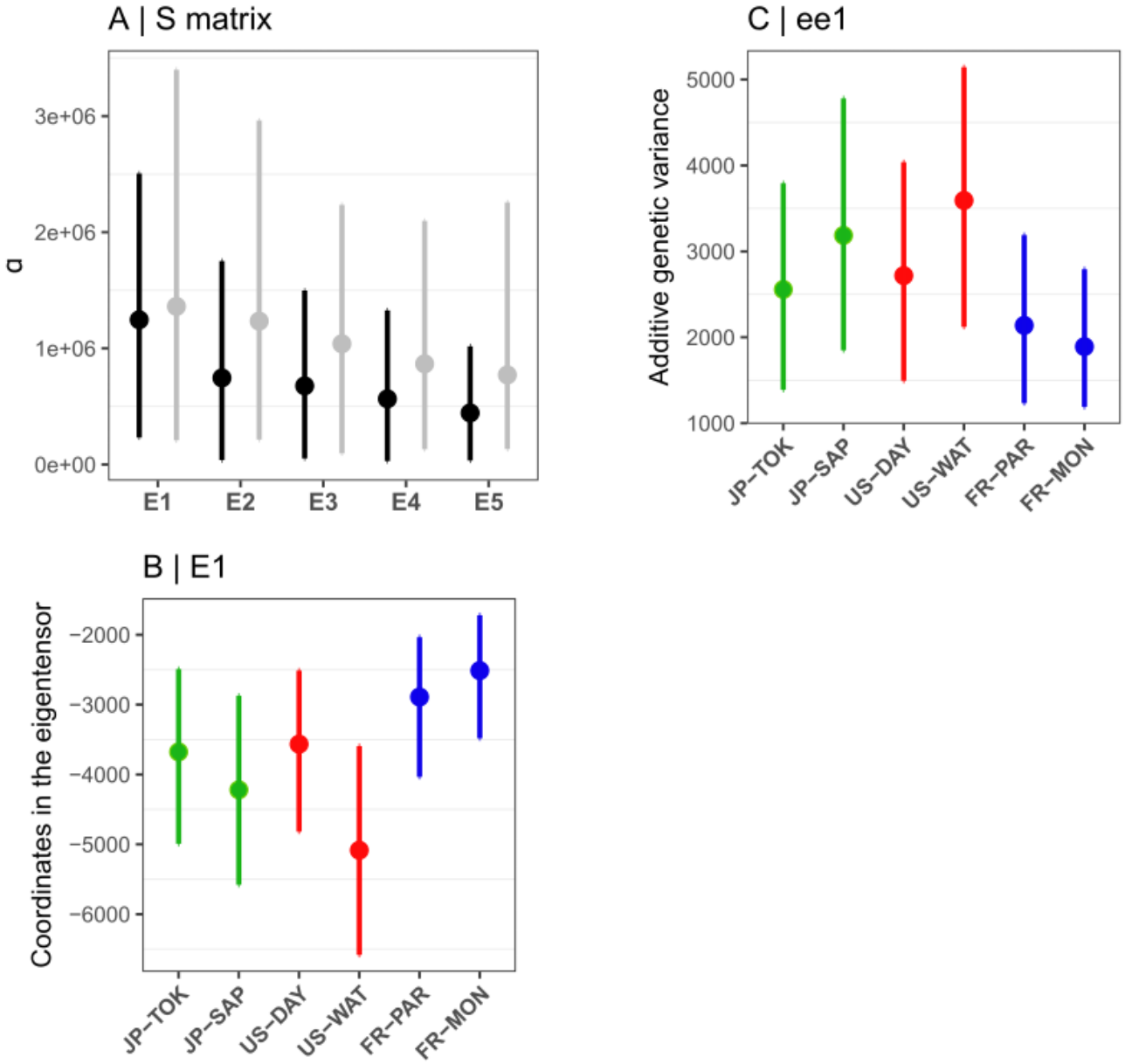

Figure 3. Results of the genetic covariance tensor analysis. A. Eigenvalues of the 5 observed eigentensors of **S** (black) are shown against the random expectation (grey). Overlapping of the confidence intervals indicates that the observed **G** matrices are not more different than a random set of **G** matrices. B. Coordinates of the **G** matrix are projected along the first eigentensor E1 for each population. This shows how each matrix contributes to the difference described by the first eigentensor E1. C. The proportion of genetic variance along the leading eigenvector of the first eigentensor (e_{11}) are shown for each population. This shows the amount of additive genetic variance along E1 for each population and overlapping of the confidence intervals indicate no significant differences between populations. In B and C, colors represent countries of origin as in Fig. 1.

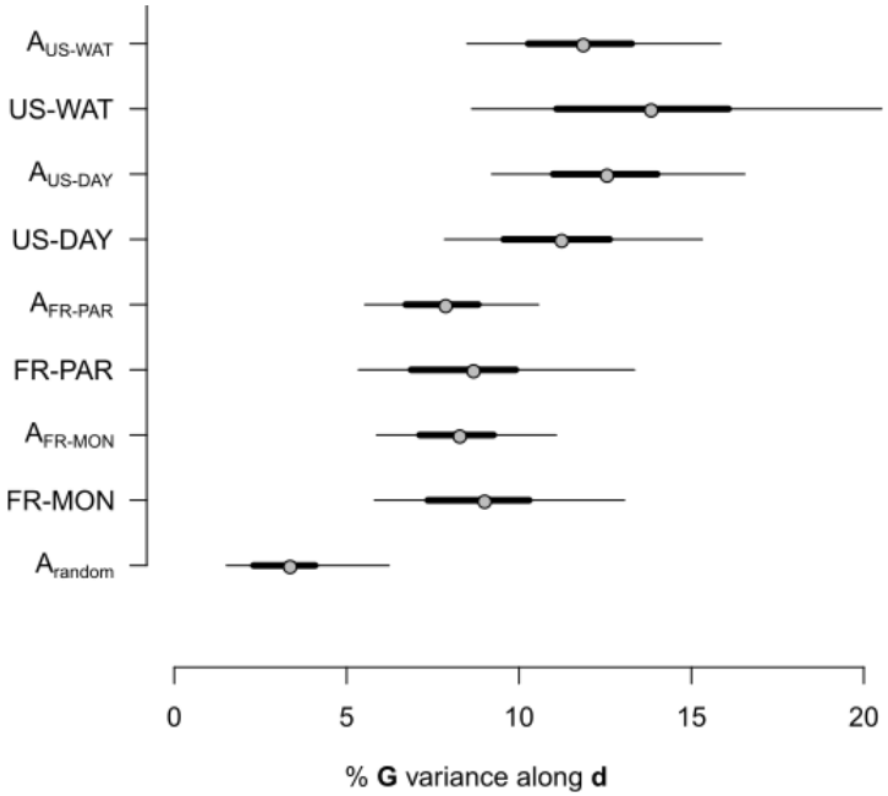

Figure 4. Percentage of genetic variance along divergence vectors. For each population, the amount of genetic variation in the direction of divergence was computed (capitalized population names) and compared to the amount of variation in the ancestral G matrix in that direction (Apop). The percentage of genetic variance along this axis is plotted (filled grey dot) with the 95% highest posterior density interval (black horizontal lines) next to the population code on the y axis. We hypothesize that selection would result in a reduction in genetic variance in the directions of divergence. This is clearly not observed, as none of the directions shows depleted genetic variance.

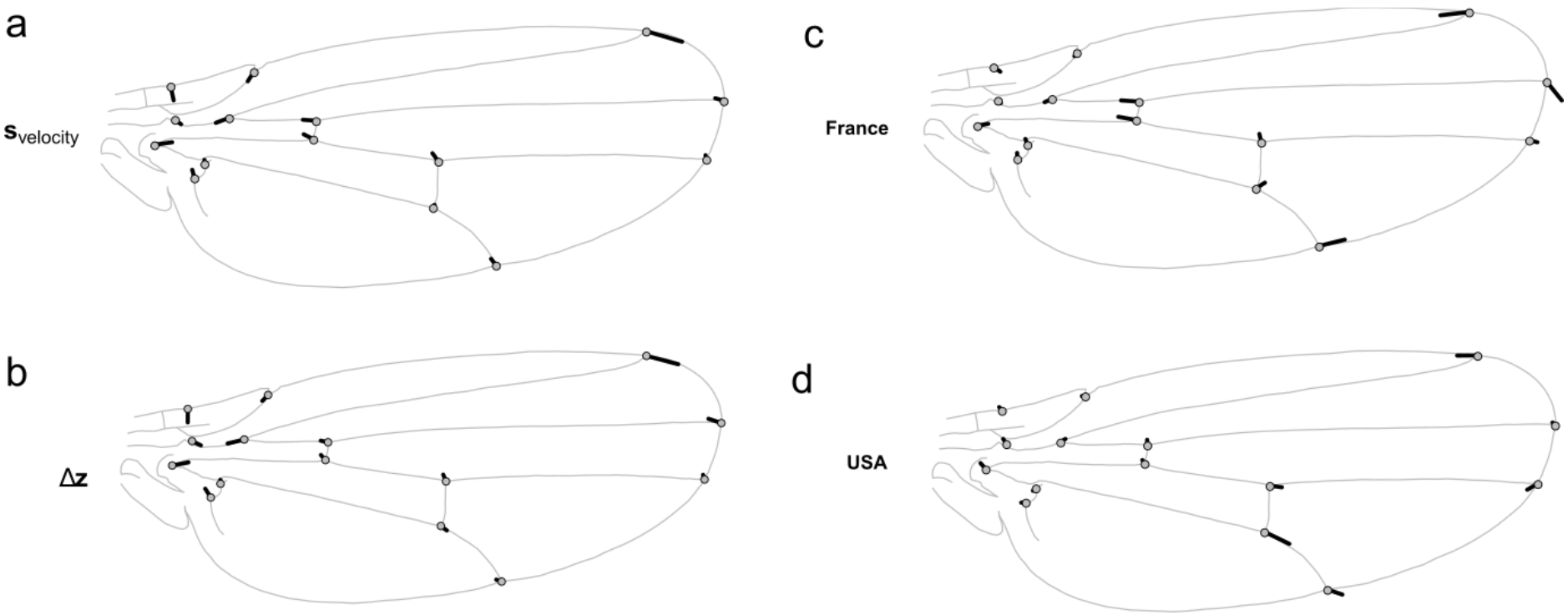

Figure 5. Response to a hypothetical selection compared to observed shape changes. Wing shape changes are displayed as vectors (black lines). a) selection differential, as defined by the shape difference between slow and fast fliers from Fraimout et al (2018). b) Average response to selection ($S_{velocity}$) based on the MCMC estimates of the ancestral **G** and **P** matrices. c) Average phenotypic divergence of the French populations from the ancestor. d) Average phenotypic divergence of the American populations from the ancestor.

Population	JP-TOK	JP-SAP	US-DAY	US-WAT	FR-PAR
JP-SAP	1.03 [0.83:1.3]				
US-DAY	0.88 [0.69:1.08]	0.87 [0.66:1.03]			
US-WAT	1.17 [0.95:1.45]	1.14 [0.9:1.38]	**1.32 [1.09:1.65]**		
FR-PAR	0.93 [0.73:1.13]	0.89 [0.7:1.07]	1.05 [0.83:1.29]]	**0.79 [0.63:0.94]**	
FR-MON	0.93 [0.73:1.11]	0.88 [0.7:1.06]	1.04 [0.83:1.26]	**0.76 [0.62:0.92]**	0.95 [0.79:1.2]

Table 1. Pairwise comparison of G matrices' volumes. For each pair of **G** matrix the posterior mode of the ratio between volumes is shown along with the Highest Posterior Density (HPD) interval. Bold values correspond to significant differences between two matrices volumes whether the ratio is significantly > 1 (row matrix is larger) or < 1 (row matrix is smaller).